APPLICATION OF SOFT COMPUTING

Multi-objective economic emission dispatch of thermal power-electric vehicles considering user's revenue

Baihao Qiao[1] · Jing Liu[1] · Jiajia Huan[2]

Abstract

In recent years, the rapid development of electric vehicles has increased the load power system and brought new challenges to the safe and stable operation of the gird. Although the vehicle-to-grid technology can reduce the load that electric vehicles put on the grid, without any incentives, electric vehicle owners are more inclined not to use vehicle-to-grid services. In this paper, therefore, a new dynamic economic emission model based on electric vehicles (DEED_EV) is proposed to maximize the electric vehicle user's revenue, as well as minimize the fuel cost and emission of the thermal power unit. In the DEED_EV model, the stochastic of electric vehicles user's travel and wear of the battery, as well as some constraints such as electric vehicles charging/discharging rate and status, electric vehicles remain power, electric vehicles travel power capacity, ramp limits, up and down reserves, and the system balance are considered. To solve the DEED_EV model, a multi-objective evolutionary algorithm based on decomposition with a step-by-step constraint handling strategy is developed. Different test cases based on the 10-unit are simulated to verify the proposed model and method. The results show that the DEED_EV model not only encourages more electric vehicles to plug into the grid but also reduces the fuel cost and emission of the thermal power unit. Besides, the electric vehicles in the DEED_EV completely realizes the peak shaving and valley filling of the load.

Keywords Dynamic power system dispatching · Electric vehicles · Multi-objective optimization · User's revenue

1 Introduction

Green, energy-saving, and environmentally-friendly electric vehicles (EVs) have developed rapidly over the past decade, thanks to people's concern about low-carbon life and the environment (Amjad et al. 2010; Farahani 2017; Lu et al. 2017). Various countries have also introduced policies to promote automobile manufacturers to develop

superior EVs and encourage users to purchase EVs, which has increased the market share of EVs year by year. According to the "Global EV Outlook 2021" published by International Energy Agency (IEA) (Admin 2021), the global stock of EVs exceeded 10 million in 2020, a 43% increase over 2019. Despite a drop in global car sales due to the Covid-19 pandemic, about 3 million EVs were sold globally in 2020. China had about 4.5 million EVs on the road by the end of 2020, the largest number in the world. It is estimated that the global EV fleet (excluding two/three-wheelers) will reach 230 million in 2030. The expanding number of EVs will continue to reduce greenhouse gas (GHG) emissions. In 2030, the global EV fleet is estimated to reduce GHG emissions by more than one-third compared to an equivalent internal combustion engine vehicles fleet. Although the development of EVs brings benefits to the environment, the use of larger-scale EVs will add additional load to the power grid, thereby affecting the safe and stable operation of the power grid. It is worth mentioning that the battery of the EV could be also used as the energy

✉ Jing Liu
  neouma@mail.xidian.edu.cn

  Baihao Qiao
  bhqiao@stu.xidian.edu.cn

  Jiajia Huan
  winnie5983@126.com

[1] Guangzhou Institute of Technology, Xidian University, Guangzhou 510555, China

[2] Power Grid Planning Research Center, China Southern Power Grid Guangdong Power Grid Co., Ltd, Guangzhou 510620, China

storage unit to store electrical energy. Moreover, EVs can be also used as a reserve energy storage unit to ensure the load demand of the system when the power supply of the generator unit is insufficient or fails. Kempton and Letendre (1997) proposed the vehicle-to-grid (V2G) technology, which allows EVs to interact with the power grid by a charging and discharging mode. Vehicles equipped with V2G services can be plugged into the grid, when they are parked at the charging station and plugged into the grid, and they can be charged or discharged (Peng et al. 2012). Therefore, the problem of EVs based on V2G services plugging into the power grid has become hot research.

Reasonable scheduling of generating units in the thermal power plant can improve the efficiency of power generation, reduce redundant power, as well as decrease the use of fossil fuels and reduce pollution emissions. The economic emission dispatch (EED) problem (Azizipanah-Abarghooee et al. 2012; Nourianfar and Abdi 2019; Xiong et al. 2022; Xu et al. 2021a) aims at decreasing the economic and emission of the thermal power plants, which is a multi-objective optimization problem (MOP). In the EED problem, the output power of each unit is simultaneously optimized to satisfy certain constraints, to minimize the economic and emissions. However, due to the different load demand in each interval, and the ramp limits of the unit, a dynamic EED (DEED) model that is more suitable for the actual dispatch scenario was proposed (Basu 2008; Guo et al. 2012; Li et al. 2021; Niknam et al. 2012). Many studies about DEED problems have been published over the past decades (Arul et al. 2015; Hu et al. 2022; Mason et al. 2017; Zhang et al. 2015). However, there are few studies considering the V2G service of EVs in the EED or DEED problems.

Saber and Venayagamoorthy (2010) proposed a V2G-based unit commitment EED model, in which EVs were being used as a small portable power plant to strengthen the security and reliability of the grid. They used particle swarm optimization (PSO) to optimize the proposed model. Yang et al. (2014) used EVs as multiple loads and analyzed the effect of EV charging on DEED. Considering the charging and discharging dispatching model of EVs (Zakariazadeh et al. 2014), the model was developed to minimize the total operating cost and emission of distribution networks. Qu et al. (2017) discussed the behavior of EV charging and discharging, developing the DEED with EVs model. Liang et al. (2019) proposed the DEED model considering EVs for peak shaving and valley filling. The bat algorithm was used to optimize the proposed DEED model and analyzed the impact of different V2G and grid to vehicle loads on DEED. Al-Bahrani et al. (2020) considered the EVs' peak shaving and valley filling in the smart city environment and developed the DEED model based on load demand management. The orthogonal PSO

was used to balance the cost and emission objective functions. Qiao and Liu (2021) considered the battery wear and proposed an economic dispatching model with EVs. Zhang et al. (2022) proposed a microgrid load scheduling model including EVs and took the minimum operation cost, pollution control cost, and load variance as the objective function. The above literature has verified from various aspects that large-scale EVs were plugged into the gird can peak shaving and valley filling for the load. However, they failed to consider the user's revenue of EVs or battery wear cost when EVs are plugged into the grid.

The user's revenue and battery wear cost determine whether users agree to take part in the V2G service. Usually, the repeated charge and discharge of the EV will cause wear of the battery. Consequently, without any incentives, it is difficult for users to actively participate in the V2G service. Therefore, in this paper, a novel DEED model based on EVs (DEED_EV) is proposed, which considers the maximization of user benefit and the minimization of fuel cost and pollution emission of the thermal unit. The purpose of the proposed DEED_EV model is to explore the optimal dispatching scheme considering three objectives simultaneously. In addition, the stochastic of the EV user's travel, and wear of the battery are considered. Some constraints such as EVs charging/discharging rate and status, EVs remain power, EVs travel power capacity, units output power and ramp limits, up and down reserves, and the system balance are included in the DEED_EV model. The framework of the DEED_EV model is illustrated in Fig. 1. From Fig. 1, the framework of the proposed DEED_EV model is divided into two components. One is the thermal power plant, and the other is the EV aggregator fleets, and they interact through the dispatch center or agency. In the power grid component, it is mainly to reduce the total fuel cost and emission by controlling the output power of the thermal power unit under the premise of ensuring load demand. However, in the EV fleets component, the charging and discharging behavior of EVs is determined according to the stochastic of the user's travel and the peak and valley state of the load.

The proposed DEED_EV is a non-convex, high-dimensional MOP with strong coupling constraints. It is hard to be solved by the conventional mathematical programming approach. In addition, the pre-handling of the constraints could reduce the calculation time and can quickly make the solutions enter the space domain to search. Therefore, according to the constraints of different components, a step-by-step adjustment constraint handling method is proposed. Firstly, the charging and discharging power in EV components is dynamically adjusted. Secondly, the output power of the thermal unit in the power grid components is adjusted to meet the power balance. Finally, the penalty function method (Qiao and Liu 2020)

Fig. 1 The framework of the proposed DEED_EV model
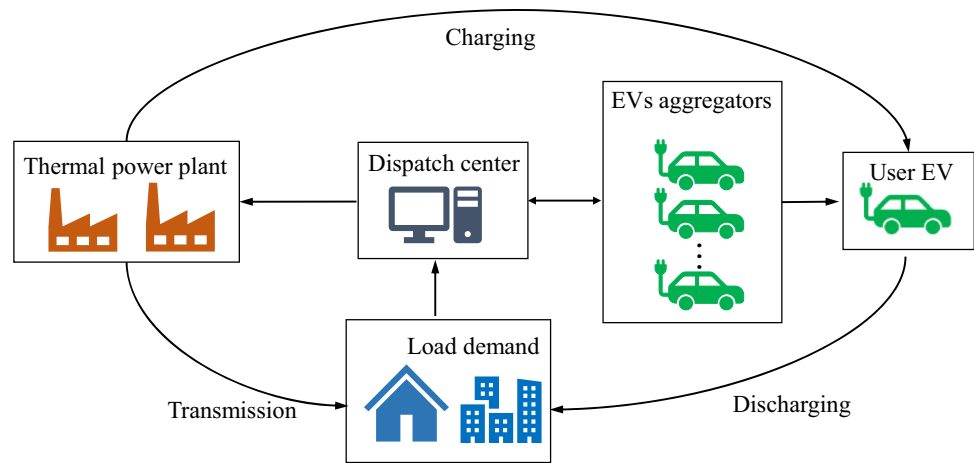
is used to weigh the objective functions to get the new objective functions.

The multi-objective evolutionary algorithm based on decomposition (MOEA/D) is developed by Zhang and Li (2007) to solve the unconstraint MOPs. Because of its superior performance in solving MOPs, MOEA/D has been applied in many fields (Gopu and Venkataraman 2019; Wang et al. 2021; Xie et al. 2022; Xu et al. 2021b; Zhu et al. 2019). In this paper, the MOEA/D with a step-by-step constraint handling method (MOEA/D-SS) is developed to solve the proposed DEED_EV problem. And four test cases based on the 10-unit system are used to verify the proposed DEED_EV model and the MOEA/D-SS method. Besides, compared with the vector evaluated particle swarm optimization (VEPSO) (Greeff and Engelbrecht 2008), multi-objective different evolution algorithm with self-adaptive parameter and local search operators based on non-dominant sorting (SaMODE_LS) (Qiao and Liu 2020), non-dominant sorting multi-objective different evolution algorithm with self-adaptive parameter (NSDESa) (Qiao et al. 2021) and dynamic NSGA-II (dNSGA-II) (Kalyanmoy et al. 2007), the performance of the MOEA/D-SS in optimizing the proposed DEED_EV with complex constraints is verified. The results show that the proposed DEED_EV model can not only reduce the fuel cost and emission of the thermal power unit but also maximize the revenue of EV users. Besides, the EV charging and discharging modes of EV obtained from the proposed model is the best compared to other modes. Moreover, the EVs in the proposed model fully realize the peak shaving and valley filling of the load. Finally, the impact of battery capital cost and electricity price on the DEED_EV model is analyzed, respectively.

The rest of this paper is organized as follows. The proposed DEED_EV model is formulated in Sect. 2. Section 3 is the pre-handling of constraints and the implementation of MOEA/D-SS in DEED_EV. The

experimental and discussion are given in Sect. 4. Finally, Sect. 5 is the conclusion.

2 Problem formulation

2.1 The stochastic model of electric vehicles

Generally, according to different usage scenarios, the uses of EVs include commercial vehicles, taxis, private vehicles, commuter vehicles, etc. Because commercial vehicles can travel at any moment, and taxis are driving almost all day. Therefore, they could not participate in V2G services and only exist in the grid as loads. However, private vehicles and commute vehicles are commonly used for daily commuting between home and the workplace. Consequently, when their owners are working or resting, they can participate in V2G services, cut the peak and fill the valley for the grid load. In this paper, the model of EVs is mainly private and commuter vehicles. For simplicity, suppose that an EV commutes only once a day; that is, there are two periods of driving, namely the periods to go to work and home. In these periods, EVs could not plug into the grid. Due to different work schedules, the commuting time of EV users is random. Let the time from home to workplace be the arrival time, and the time from workplace to home be the departure time. Based on the US National Household Travel Survey (NHTS 2017), the stochastic of EVs arrival time and departure time can be modeled with a normal distribution (Lu et al. 2018; Mohiti et al. 2019), respectively.

$$F_a(t) = \frac{1}{\sigma_a \sqrt{2\pi}} e^{-\frac{(t-\mu_a)^2}{2\sigma_a^2}}, \quad 0 < t \le 24 \tag{1}$$

$$F_d(t) = \frac{1}{\sigma_d \sqrt{2\pi}} e^{-\frac{(t-\mu_d)^2}{2\sigma_d^2}}, \quad 0 < t \le 24 \tag{2}$$

where σ_a and σ_d are the variances of the arrival time and departure time. μ_a and μ_d are the means of the arrival time and departure time, respectively.

2.2 Battery wear model

The heart that drives an EV is the battery component. The battery lifetime determines the key factor for whether the user intends to buy an EV, and it also directly affects the user's time limit for using the EV. More importantly, it is also a key factor that determines EV users' participation in V2G services. Therefore, it is necessary to study the battery wear when EVs participate in grid V2G services. At present, there are three battery technologies, lead-acid, nickel-metal hydride, and lithium-ion, that are used most in the market (Zhou et al. 2011). These technologies have different advantages in capability, safety, life, and cost. In the same case, lithium-ion technology is widely used by automobile manufacturers because of its high-power density (Gonzalez-Castellanos et al. 2020). For simplicity, the EVs are driven by lithium-lion in this paper. The service life of the battery will degrade with calendar aging and cycling, which is mainly caused by irreversible electro-chemical side reactions. This will result in a reduction in battery capacity, and the battery needs to be replaced to ensure the normal users of the EV when reduced to the standard threshold. Calendar life represents the expected life of the battery, while cycle life is usually expressed by the number of charge/discharge cycles (Wang et al. 2016). In this paper, the revenues of a charge and discharge cycle of EV users are considered, so only the battery wear caused by the cycle is analyzed.

The cycle life of the battery is related to ambient temperature and discharge of depth (DoD). However, the researchers have shown that compared to other technology, the effect of ambient temperature on lithium-ion is less obvious (Zhou et al. 2011). In this paper, the ambient temperature is reasonably ignored, and only the impact of DoD on battery wear is analyzed. The DoD refers to the absolute discharge relative to the rated battery capacity, denoted by D_{od}, which is related to the state of charge (SoC). The relationship between battery cycle life and D_{od} is defined as follows.

$$Ln(L) = -0.795Ln(D_{od}) + 6.5425 \tag{3}$$

where L is the number of battery cycles under D_{od}. (3) can be transformed into

$$L = 694D_{od}^{-0.795} \tag{4}$$

The D_{od} can be calculated by SoC. Therefore, during discharge, D_{od} at time t within a cycle is defined as Eq. (5), which is illustrated in Fig. 2a.

$$D_{od}^t = SoC(t-1) - SoC(t), \quad 0 < t \le 24 \tag{5}$$

where SoC (0) = 1 means that the initial SoC is 100%. Figure 2(b) shows that the battery cycle life goes down with increasing D_{od}. When each D_{od} of the battery is 20%, the cycle life of the battery is approximately 2494. However, when the battery is fully discharged (D_{od} is 100%) each time, its cycle life is only 694. Therefore, the appropriate D_{od} of the battery can ensure that EVs have a long service life.

2.3 Modeling of dynamic economic emission dispatch with electric vehicles

In this subsection, the DEED_EV model is proposed to minimize the fuel cost and the population emission of the thermal power units as well as maximize the revenues of the EVs user. In the proposed DEED_EV model, the EVs battery wear cost and the user's travel stochastic are included. And some constraints such as system power balance, EVs remain power, users travel, ramp rates and spinning reserve are considered.

2.3.1 Objective functions

(1) Fuel cost

The fuel cost of thermal power units is defined in the form of a quadratic function (Han et al. 2001; Qiao and Liu 2020).

$$\text{Minimize } F_C = \sum_{t=1}^{T} \sum_{i=1}^{N} (a_i + b_i P_{i,t} + c_i P_{i,t}^2) \tag{6}$$

where T and N are the dispatching period and number of units, respectively. a_i, b_i and c_i are the coefficients of the ith unit, and $P_{i,t}$ is the dispatchable power of the ith unit at time t.

(2) Emission

The emission of thermal power units is defined as the sum of the quadratic function and exponential function (Qu et al. 2018).

$$\text{Minimize } F_M = \sum_{t=1}^{T} \sum_{i=1}^{N} [(\alpha_i + \beta_i P_{i,t} + \gamma_i P_{i,t}^2 + \zeta_i exp(\varphi_i P_{i,t})] \tag{7}$$

where α_i, β_i, γ_i, ζ_i and φ_i are the emission coefficients of the ith unit.

(3) EVs users' revenues

When EVs participated in V2G services, certain revenues will be generated. And the higher the revenue, the
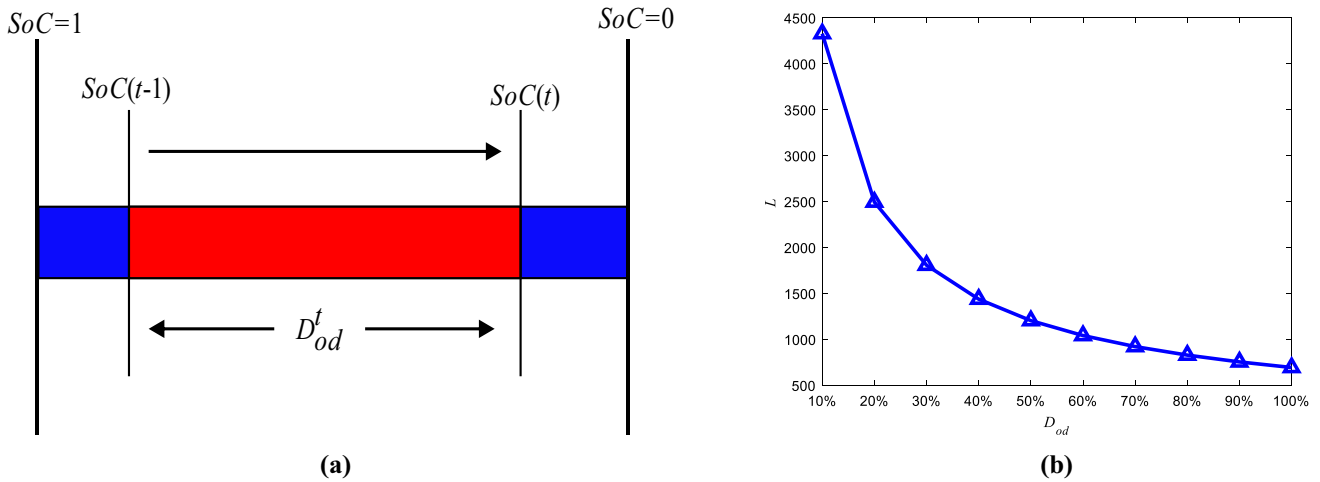
Fig. 2 Definitions of the D_{od} and cycle life. **a** The relationship between D_{od} and SOC, and **b** The relationship between D_{od} and the cycle of life

more incentives users will add their EVs to the V2G services. The user's revenue is defined as follows.

$$\text{Maximum } F_R = \sum_{t=1}^{T} \sum_{i=1}^{N_{ev}} (P_{Dch,i}^t \pi_t - P_{Ch,i}^t \pi_t - P_{Dch,i}^t \pi_{bd}) \tag{8}$$

where the first term is the income from EVs discharge. The second term is the cost of charging EVs. The last term is the cost of battery wear caused by the discharge. N_{ev} is the number of EVs. $P_{Dch,i}^t$ and $P_{Ch,i}^t$ are the discharging and charging of the ith EVs at time t, respectively. π_t is the electricity price at time t. π_{bd} is the battery wear cost which can be calculated as follows.

$$\pi_{bd} = \frac{C_{ev}}{LE_{cap}D_{od}} \tag{9}$$

where C_{ev} is the battery capital cost in \$/kWh. E_{cap} is the battery capacity.

2.3.2 Constraints

The DEED_EV problem is subjected to some technology constraints which are described as follows.

(1) Constraints of EVs

$$0 \leq P_{Ch}^t \leq \overline{P_{Ch}^t} u_{Ch}^t, \quad t \in [t_{arr}, t_{dep}] \tag{10}$$

$$0 \leq P_{Dch}^t \leq \overline{P_{Dch}^t} u_{Dch}^t, \quad t \in [t_{arr}, t_{dep}] \tag{11}$$

$$u_{Ch}^t + u_{Dch}^t = 1, \quad t \in [t_{arr}, t_{dep}] \tag{12}$$

$$u_{Ch}^t + u_{Dch}^t = 0, \quad t \notin [t_{arr}, t_{dep}] \tag{13}$$

$$R_t = R_{t-1} + \lambda_C P_{Ch,t} \Delta t - \frac{1}{\lambda_D} P_{Dch,t} \Delta t - S_{Trip,t} \tag{14}$$

$$\underline{SoC}E_{cap} \leq R_t \leq \overline{SoC}E_{cap} \tag{15}$$

$$\sum_{t=1}^{T} S_{Trip,t} = \sum_{t=1}^{T} \lambda_C P_{Ch,t} \Delta t - \sum_{t=1}^{T} \frac{1}{\lambda_D} P_{Dch,t} \Delta t \tag{16}$$

where $\overline{P_{Ch}^t}$ and $\overline{P_{Dch}^t}$ are the maximum charging and discharging of the EV at time t. u_{Ch}^t and u_{Dch}^t are binary variables representing the charging and discharging state of the battery. t_{arr} and t_{dep} represent the arrival time and departure time. $\underline{SoC}$ and $\overline{SoC}$ are the minimum and maximum SoC. R_t is the remaining power of the EVs at time t. λ_C and λ_D are the charging and discharging efficiencies. Δt is the dispatch interval and set to 1 in this paper. $S_{Trip,t}$ is the power consumed in driving EVs at time t, and $S_{Trip,t} = \Delta SL_d$, where ΔS is the average power consumption of EV driving and L_d is the driving distance. Equations (10) and (11) are the charging and discharging constraints of EVs, which indicates that EVs could not be overcharged and over-discharged. Equation (12) indicates that charging and discharging could not be performed simultaneously. Equation (13) represents not participating in V2G when EV is driving. The remaining power calculation and constraint are Eqs. (14) and (15), respectively. Equation (16) represents the travel constraint of EVs, which ensures that EVs have sufficient travel power.

(2) Constraints of power system

$$\underline{P_{i,t}} \leq P_{i,t} \leq \overline{P_{i,t}} \tag{17}$$

$$\sum_{t=1}^{N} P_{i,t} + \sum_{i=1}^{N_{ev}} P_{Dch,i}^t = P_{D,t} + P_{L,t} + \sum_{i=1}^{N_{ev}} P_{Ch,i}^t \tag{18}$$

$$P_{L,t} = \sum_{i=1}^{N} \sum_{j=1}^{N} P_{i,t} B_{ij} P_{j,t} + \sum_{i=1}^{N} P_{i,t} B_{i0} + B_{00} \tag{19}$$

$$\begin{cases} P_{i,t} - P_{i,t-1} \leq U_{Rt}\Delta t \\ P_{i,t-1} - P_{i,t} \leq D_{Rt}\Delta t \end{cases} \qquad (20)$$

$$\sum_{i=1}^{N} \min\left(\min\left(\overline{P_{i,t}}, P_{i,t-1} + U_{Rt}\Delta t\right) - P_{i,t}, \frac{U_{Rt}}{6}\right)$$

$$\geq S_{R,t}^{u} + \vartheta_u \sum_{i=1}^{N_{ev}} \left(P_{Dch,i}^{t} + P_{Ch,i}^{t} \right) \qquad (21)$$

$$\sum_{i=1}^{N} \min\left(\underline{P_{i,t}} - \max\left(\underline{P_{i,t}}, P_{i,t-1} - D_{Rt}\Delta t\right), \frac{D_{Rt}}{6}\right)$$

$$\geq \vartheta_d \sum_{i=1}^{N_{ev}} \left(P_{Dch,i}^{t} + P_{Ch,i}^{t} \right) \qquad (22)$$

where $\underline{P_{i,t}}$ and $\overline{P_{i,t}}$ are the minimum and maximum power of the ith unit, respectively. $P_{D,t}$ is the load demand. $P_{L,t}$ is the system loss at time t, which is calculated by Eq. (19), and B_{ij}, B_{i0}, and B_{00} are the coefficients. U_{Rt} and D_{Rt} are the increase and decrease rates at time t. $Su R,t$ is the up spinning reserve at time t. ϑ_u and ϑ_d are the reserve coefficients of EVs, respectively. Equation (17) is the output limit of the thermal power unit. Equation (18) is the power balance constraint of the system. Equation (20) is the up and down ramp constraints, which indicates that the power change in adjacent intervals could not exceed the set threshold. The system's up and down reserve constraints are defined as Eqs. (21) and (22), which means that the generator is conked or the power supply is interrupted, and the system can respond quickly to maintain the continuity of the grid power supply.

3 Implementation of MOEA/D-SS for dynamic economic emission dispatch with electric vehicles

3.1 Constraint handling method

The proposed DEED_EV model has three objective functions, which are to minimize fuel cost and emission of the thermal power unit and maximize the user's revenue. To optimize these three objective functions at the same time, the function of the user's revenue Eq. (8) is transformed into the form of minimum $F'_R=1/F_R$. Therefore, the optimization of the DEED_EV problem could be transformed into the following form:

$$\begin{cases} \text{Minimize} & [F_C, F_M, F'_R] \\ \text{Subject to} & \text{Constraints } (10) - (22) \end{cases} \qquad (23)$$

There are many constraints in the proposed DEED_EV model, and these constraints are highly coupled. Therefore, if the constraints are not processed in advance, infeasible solutions will be generated, which will lead to difficulty in optimization and a waste of calculation time. The constraint handling method with the step-by-step adjustment is adopted in this paper, and the detailed processes are given as follows.

When EVs participate in V2G services, they must always be plugged into the grid except for the driving, and there should be enough power for the users to travel. Therefore, the travel constraint (16) in constraints of EVs should be adjusted first. The detailed adjustment process for EVs constraints is shown in Algorithm 1. Lines 1 and 2 are operations before constraints adjustment. Lines 3–14 are step-by-step adjustment operations. When the adjustment of $P_{Ch,t}$ and $P_{Dch,t}$ is completed (lines 8 and 9), judge whether it is out of bounds (lines 10 and 11). Finally, when the k and $|\text{vilo}_{ev}^k|$ meet the preset threshold (K_{ev} and ε_{ev}), the adjustment is terminated (lines 5–7). After performing Algorithm 1, new $P_{Ch,t}$, $P_{Dch,t}$ and $|\text{vilo}_{ev}^k|$ will be output, and then Eq. (14) constraint violation vilo_R will be calculated.

Algorithm 1: EVs Constraint Handling Procedure

Input:
> $P_{Ch,t}$, $P_{Dch,t}$: Charging and discharging of EVs;
> K_{ev}, ε_{ev}: Maximum adjustment and the threshold value of EVs;

Output:
> Adjusted $P_{Ch,t}$, $P_{Dch,t}$, and $|vilo_{ev}^k|$;

1:    $k \leftarrow 0$;

2:    $vilo_{ev}^k = \sum_{t=1}^{T} S_{Trip,t} - \left(\sum_{t=1}^{T} \lambda_C P_{Ch,t}\Delta t - \sum_{t=1}^{T} \frac{1}{\lambda_D} P_{Dch,t}\Delta t \right)$ (24);

3:    **while** $k < K_{ev}$ **do**

4:      **repeat**

5:        **if** $k > K_{ev}$ **or** $|vilo_{ev}^k| \leq \varepsilon_{ev}$ **then**

6:          **break**;   % End constraint adjustment

7:        **end if**;

8:        $P_{Ch,t} = P_{Ch,t} + vilo_{ev}^k/T$;

9:        $P_{Dch,t} = P_{Dch,t} - vilo_{ev}^k/T$;

10:      $P_{Ch,t} = \min(P_{Ch,t}, P'_{Ch}u_{Ch}^t)$;

11:      $P_{Dch,t} = \min(P_{Dch,t}, P'_{Dch}u_{Dch}^t)$;

12:      Update $vilo_{ev}^k$ according to (24);

13:      $k \leftarrow k+1$;

14:   **end while**;

When the EVs constraint handling is completed, new $P_{Ch,t}$ and $P_{Dch,t}$ are added to the constraint handling of the power system. The constraint handling procedure of the power system is shown in Algorithm 2, in which the loss $P_{L,t}$ is calculated first (line 2), and then the value vilo_P^k to be adjusted is obtained (line 3). Through iterative adjustment (lines 4–24), the dynamic update of $P_{i,t}$ (lines 9–20) is realized. However, when the adjustment is completed

(lines 9–13), it is necessary to further determine whether $P_{i,t}$ crosses the boundary (lines 14–20).

Algorithm 2: Power System Constraint Handling Procedure

Input:

       $P_{i,t}$: Output power of thermal power units;

       $P_{Ch,t}$, $P_{Dch,t}$: Charging and discharging of EVs;

       N: The number of thermal power units;

       K_P, ε_P: Maximum adjustment and the threshold value of the power system;

Output:

       Adjusted $P_{i,t}$ and $|vilo_P^k|$;

1:    $k \leftarrow 0$;

2:    Get $P_{L,t}$ according to (19);

3:    $vilo_P^k = \sum_{t=1}^{N} P_{i,t} + \sum_{i=1}^{N_{ev}} P_{Dch,i}^t - \left(P_{D,t} + P_{L,t} + \sum_{i=1}^{N_{ev}} P_{Ch,i}^t \right)$ (25);

4:    ***while*** $k < K_P$ ***do***

5:       ***repeat***

6:       ***if*** $k > K_P$ ***or*** $|vilo_P^k| \leq \varepsilon_P$ ***then***

7:          ***break;***   *% End constraint adjustment*

8:       ***end if***;

9:       ***if*** $vilo_P^k < 0$ ***then***

10:       $P_{i,t} = P_{i,t} + |vilo_P^k|/N$;

11:       ***else***

12:       $P_{i,t} = P_{i,t} - vilo_P^k/N$;

13:       ***end if***;

14:       ***if*** $t = 1$ ***then***

15:       $P_{i,t} = \min(P_{i,t}, \overline{P_{i,t}})$;

16:       $P_{i,t} = \max(P_{i,t}, \underline{P_{i,t}})$;

17:       ***else***

18:       $P_{i,t} = \min(P_{i,t}, \min(P_{i,t-1} + U_{Rt}, \overline{P_{i,t}})$;

19:       $P_{i,t} = \max(P_{i,t}, \max(P_{i,t-1} - D_{Rt}, \underline{P_{i,t}})$;

20:       ***end if***

21:    Update $P_{L,t}$ according to (19);

22:    Update $vilo_P^k$ according to (25);

23:    $k \leftarrow k+1$;

24: ***end while***;

After performing Algorithm 2, new $P_{i,t}$ and $|vilo_P^k|$ will be output, and then calculate Eqs. (21) and (22) constraint violations $vilo_u$ and $vilo_d$. Therefore, the proposed DEE-D_EV model total constraint violations $vilo = |vilo_{ev}^k| + |vilo_R| + |vilo_P^k| + |vilo_u| + |vilo_d|$. The multi-objective problem with constraint (23) is transformed into an unconstrained optimization problem (26) through the penalty function method (Ding et al. 2015). It is obvious that when $vilo = 0$ all objective functions are minimum, and the corresponding solutions are the feasible solutions.

$$\text{Minimize } F_j = F_Q + s \cdot vilo, \quad j, Q = C, M, R \qquad (26)$$

where s is the penalty coefficient.

3.2 Implementation of MOEA/D-SS in DEED_EV

MOEA/D has been proved to have a very significant effect in solving unconstrained MOPs. In order to optimize the proposed DEED_EV model with strong constraints, MOEA/D-SS is developed by combining the step-by-step constraint handling method with MOEA/D. In MOEA/D-SS, the decomposition method of Tchebycheff is adopted to decompose the MOP into a series of subproblems and optimize the subproblems to obtain the final solutions.

Different from the method of generating weight vectors for two objectives, here, the Latin hypercube sample method is used to generate weigh vectors for three objectives. The specific procedure of implementation of MOEA/D-SS in DEED_EV is shown in Algorithm 3. Lines 1–8 are the initialization process of MOEA/D-SS, and its detailed iterative operations are lines 9–19. Besides, the flowchart of the proposed MOEA/D-SS to optimize the DEED_EV problem is shown in Fig. 3. G_{enmax} and g_{en} represent the maximum number of iterations and the number of iterations.

The computational complexity of MOEA/D-SS is analyzed as follows. The major computational costs of Algorithm 1 are to calculate $P_{Dch,i}^t$ and $P_{Ch,i}^t$ by Eq. (16). Therefore, the total computational complexity of Algorithm 1 is $O(K_{ev}\log N)$. In the same way, the computational costs of Algorithm 2 are to calculate $P_{i,t}$ and $P_{L,t}$ by Eqs. (18) and (19), and its computational complexity is $O(K_p\log N)$ and $O(2K_p\log N)$, respectively. The total computational complexity of Algorithm 2 is $O(K_p\log N)$. The computational costs of MOEA/D are to generate Np trial

---

Algorithm 3: MOEA/D-SS Implemented in DEED_EV

Input:
  DEED_EV problem parameters and a termination criterion;
  Np: Population size;
  $\lambda^1, \lambda^2, \dots, \lambda^{Np}$: Np weight vectors;
  T: The number of weight vectors in the neighborhood of $\lambda^1, \lambda^2, \dots, \lambda^N$;
  DE parameters: Scaling factor (F) and crossover rate (CR);

Output:
  Dispatch solutions (final $[P^1,\dots, P^{Np}]^T$ and $[F_C(P^i), F_M(P^i), F_R^{'}(P^i)]^T$);

1: **Initialize:**
2:   Generate $Np\times m$ (m: Number of objective functions) weight vectors by Latin hypercube sample method;
3:   Calculate the Euclidean distances between any two weight vectors;
4:   Find out T closets weight vectors from $Np\times m$ weight vectors, for each $i = 1, 2,\dots, Np$, set neighboring $B(i) = (i_1,\dots, i_T)$, therefore, $\lambda^{i_1},\dots,\lambda^{i_T}$ are the T closest weight vectors to λ^i;
5:   Random generation of initial population $P^1,\dots, P^{Np}$; Initialize the reference point $z = (z_1,\dots, z_m)^T$;
6:   Repair P^i according to Algorithms 1 and 2;
7:   Compute objective functions: $F_j(P^i)$, $j = C, M, R$;
8:   Update z: if $z_j < F_j(P^i)$, then set $z_j = F_j(P^i)$;
9: **Iterations:**
10:   **while** (*termination criteria are not satisfied*) **do**
11:     Evolve by DE operators;
12:     **for** $i = 1$ **to** Np **do**
13:       Randomly select three indexes r_1, r_2, r_3 inequal i from B(i); and then obtain a new P^i from P^{r_1}, P^{r_2}, P^{r_3} by using DE operator DE/rand/1;
14:       Repair new P^i by the variable boundary ($\underline{P_{i,t}}$, $\overline{P_{i,t}}$, $\overline{P_{Ch}^t}$, and $\overline{P_{Dch}^t}$), and further change its diversity by mutation operator in genetic operations;
15:       Perform lines 6-8 in initialization to update P^i and z;
16:       Update of neighboring solutions, for each $l \in B(i)$, if $g^{te}(P^i \mid \lambda^l, z) \leq g^{te}(P^l \mid \lambda^l, z)$, then set $P^l = P^i$, where g^{te} represents Tchebycheff method, and minimize $g^{te}(P^i \mid \lambda^l, z) = \max_{1\leq j\leq m}\{\lambda_j \mid F_j(P^i)\text{-}z_j\}$;
17:       **end for**
18:     If the termination criteria are satisfied, then stop and output $[P^1, P^2,\dots, P^{Np}]^T$, and $[F_C(P^i), F_M(P^i), F_R^{'}(P^i)]^T$, $i = 1, 2, \dots, Np$. Otherwise, go to line 10;
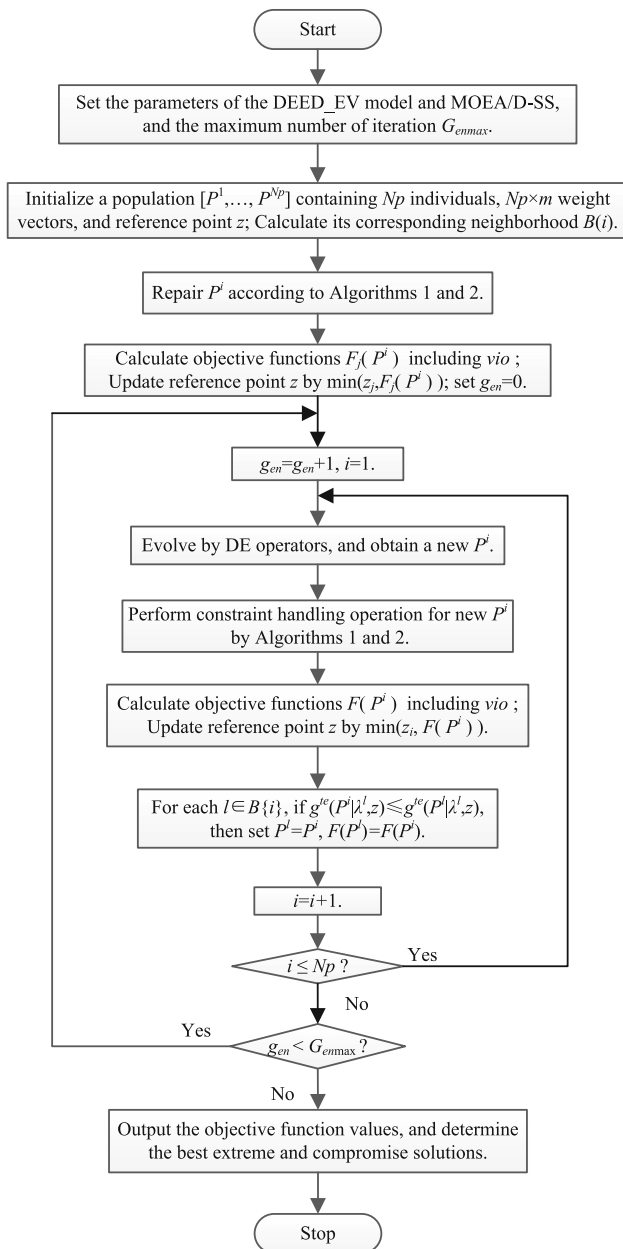19:   **end while**;

Fig. 3 The flowchart of MOEA/D for DEED_EV

Table 1 The EVs parameters

E_{cap}(kW·h)	C_{ev} ($/kW·h)	$\overline{P_{Ch}^t}$, $\overline{P_{Dch}^t}$, $\underline{SoC}$	$\overline{SoC}$
24	0.50	0.2 E_{cap}	1 E_{cap}
ΔS(kW·h/km)	L_d(km)	λ_C, λ_D	ϑ_u, ϑ_d
0.15	25	0.9	0.3

solutions, the computational complexity of MOEA/D is (mTN), where m is the number of the objective functions and T is the dimensional of close weight. Therefore, the computational complexity of MOEA/D-SS is $O(mTN)$.

4 Experimental results and discussion

In this section, four test cases based on the 10-unit system are used to demonstrate the availability of the proposed DEED_EV model and the performance of the MOEA/D-SS. The thermal power unit parameters and load demand are given in (Qiao and Liu 2020) and (Basu 2014). Assuming that all EVs in the model are the same type, and all times are participated in V2G service dispatching except the driving periods. In addition, let each EV have an SoC of 100% before the start of the first commute time, that is, the EV is full power before daily use. Therefore, SoC(1) = 100%, and the SoC(2) = $1 - L_d/L_d^{max}$, L_d^{max} is the maximum driving distance when SoC is 100%. The EV parameters are listed in Table 1. Due to the $\overline{P_{Ch}^t}$ and $\overline{P_{Dch}^t}$ are $0.2E_{cap}$, the D_{od} is 0.8 of each EV. $Su\ R,t$ is set to $0.1P_{D,t}$, and one dispatch is 24 h. K_{ev} and K_P are both set to 10, s is set to 100. ε_{ev} and ε_P are set to 1e − 6. μ_a and μ_d are set to 8 and 18, respectively. σ_a and σ_d are set to 1. The load demand $P_{D,t}$ (Qiao and Liu 2020) and electricity price π_t (Zakariazadeh et al. 2014) are shown in Fig. 4. All tests are performed in MATLAB 2019a environment on a PC with Core I5-6500 CPU, 8G RAM. In each case, the iteration is set to 3000, and the Np is set to 300. Each algorithm runs independently 31 times and records the corresponding results.

4.1 Case 1

In this case, the 10-unit system with 50,000 EVs is simulated to verify the proposed MOEA/D-SS. In order to further demonstrate the performance of MOEA/D-SS, the VEPSO (Greeff and Engelbrecht 2008), SaMODE_LS (Qiao and Liu 2020), NSDESa (Qiao et al. 2021), and dNSGA-II (Kalyanmoy et al. 2007) are compared with it.
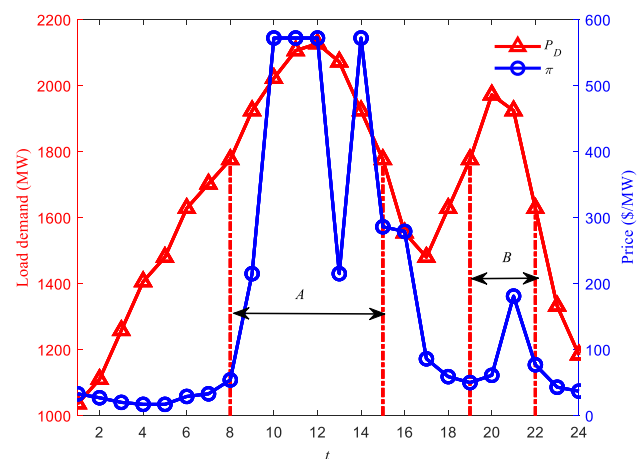

Fig. 4 The profiles of the load demand and electricity price. A and B are two different peak load periods

Table 2 The median solution of all algorithms

Indicator	Methods	Cost ($)	Emission (lb)	Revenue ($)
Median	VEPSO	2.4401E + 06	3.0897E + 05	2.6348E + 05
		2.4961E + 06	2.8999E + 05	2.8034E + 05
		2.5355E + 06	3.0582E + 05	3.0841E + 05
	dNSGA-II	2.4325E + 06	2.8922E + 05	2.6103E + 05
		2.4727E + 06	2.8299E + 05	2.5343E + 05
		2.5389E + 06	3.1148E + 05	3.8288E + 05
	NSDESa	2.4127E + 06	2.9273E + 05	3.5182E + 05
		2.4635E + 06	2.8134E + 05	3.4092E + 05
		2.4956E + 06	2.9856E + 05	4.5211E + 05
	SaMODE_LS	2.4057E + 06	2.9227E + 05	3.9228E + 05
		2.4795E + 06	2.7846E + 05	4.6141E + 05
		2.4919E + 06	2.7762E + 05	**4.6433E + 05**
	MOEA/D-SS	**2.3916E + 06**	2.8672E + 05	3.2696E + 05
		2.4770E + 06	**2.7323E + 05**	3.0125E + 05
		2.4099E + 06	2.8362E + 05	3.2271E + 05

Table 3 The evaluation indicators of the objective functions obtained by all algorithms

Indicators	Methods	Cost ($)	Emission (lb)	Revenue ($)
Best	VEPSO	2.4705E + 06	2.8684E + 05	3.4110E + 05
	dNSGA-II	2.4559E + 06	2.8144E + 05	4.1790E + 05
	NSDESa	2.4003E + 06	2.7784E + 05	4.6770E + 05
	SaMODE_LS	2.3828E + 06	2.7484E + 05	**4.9607E + 05**
	MOEA/D-SS	**2.3807E + 06**	**2.7090E + 05**	3.5203E + 05
Worst	VEPSO	2.4817E + 06	2.9249E + 05	2.7751E + 05
	dNSGA-II	2.4143E + 06	2.9154E + 05	3.2952E + 05
	NSDESa	2.4347E + 06	2.8401E + 05	4.2707E + 05
	SaMODE_LS	2.4305E + 06	2.8257E + 05	**4.5074E + 05**
	MOEA/D-SS	**2.4065E + 06**	**2.7465E + 05**	2.7350E + 05
Avr	VEPSO	2.4430E + 06	2.9071E + 05	3.0533E + 05
	dNSGA-II	2.4328E + 06	2.8473E + 05	3.8664E + 05
	NSDESa	2.4384E + 06	2.8506E + 05	3.7636E + 05
	SaMODE_LS	2.4534E + 06	2.8017E + 05	**4.4575E + 05**
	MOEA/D-SS	**2.3928E + 06**	**2.7307E + 05**	3.1601E + 05
Std	VEPSO	1.9246E + 04	3.2579E + 03	2.0707E + 04
	dNSGA-II	1.1691E + 04	3.3955E + 03	2.6531E + 04
	NSDESa	7.5046E + 03	1.5181E + 03	**1.0885E + 04**
	SaMODE_LS	1.1397E + 04	1.7471E + 03	1.1272E + 04
	MOEA/D-SS	**6.2493E + 03**	**8.9455E + 02**	2.2732E + 04

The median value of the minimum values of each objective function obtained by all algorithms is listed in Table 2. The minimum value of the objective function obtained by each algorithm is the extreme solution of the objective function, and the corresponding row indicates the values of other objective functions under this value. Besides, in this paper, the best values are highlighted in bold. It can be seen from Table 2, in terms of the median value, dispatching solutions obtained by SaMODE_LS and NSDESa can maximize users' revenue. However, in terms of the cost and emission

of the objective function, the median value of the optimal value obtained by the proposed MOEA/D-SS is the best compared with those of other algorithms. Besides, although dNSGA-II (3.8288E + 05) obtained those users' revenue 18.65% higher than MOEA/D-SS (3.2271E + 05). However, the cost and the emission decreased by 5.75% and 9.82%, respectively, compared with MOEA/D-SS. Therefore, for the median indicator, the performance of the proposed MOEA/D-SS is better than those of other

Table 4 The best compromise obtained by five algorithms

Methods	Cost ($)	Emission (lb)	Revenue ($)
VEPSO	2.4450E + 06	2.9075E + 05	3.1840E + 05
dNSGA-II	2.4276E + 06	2.8430E + 05	3.0568E + 05
NSDESa	2.4268E + 06	2.8351E + 05	3.6657E + 05
SaMODE_LS	2.4416E + 06	2.8218E + 05	**4.0368E + 05**
MOEA/D-SS	**2.4145E + 06**	**2.7913E + 05**	3.2883E + 05
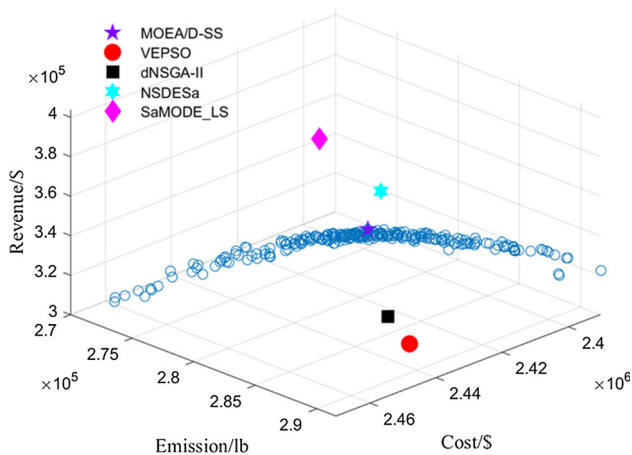
Fig. 5 The MOEA/D-SS Pareto front and five algorithms best compromise

algorithms and only slightly worse than those of SaMO-DE_LS and NSDESa in terms of user's revenue.

The evaluation indicators such as the best and worst of the objective functions, as well as the average (Avr) and standard deviation (Std) of the best value, are listed in Table 3. From Table 3, compared with VEPSO, dNSGA-II, and NSDESa, the corresponding objective function value of the dispatch solutions obtained by SaMODE_LS is the best among all indicators. However, in the best, worst, and Avr indicators corresponding to objective functions cost and emission, the proposed MOEA/D-SS is superior to SaMODE_LS. Besides, among the three objective functions, MOEA/D-SS only performs worse than SaMO-DE_LS on objective function user revenue. The same conclusion above can be also drawn from the best compromise solution, and the best compromises obtained by five algorithms are shown in Table 4.

The Pareto front of MOEA/D-SS and the best compromise of the five methods are illustrated in Fig. 5. It is obvious that those results obtained by MOEA/D-SS are superior to those of other methods. Consequently, the MOEA/D-SS's performance is better than that of VEPSO and dNSGA-II's and, in terms of the objective functions of the cost and emission, is better than NSDESa and

SaMODE_LS. The best compromise solutions obtained by MOEA/D-SS are given in Table 5, and the negative in the V2G item indicates EV charging. Besides, constraints checking for the compromise solution are shown in Fig. 6, which shows that the dispatch solution obtained by MOEA/D-SS satisfies the power balance.

4.2 Case 2

The different charging and discharging control behavior are studied in this case. In case 1, the charging and discharging modes are smartly selected, and the system intelligently selects the charging or discharging time according to the load. The charging and discharging time are fixed according to different peak loads. In the fixed scenario, let the EVs perform discharge operation during the peak periods of the load, that is, the periods included in A and B in Fig. 4. Then charge it during periods other than A and B. The median of results is listed in Table 6. It is obvious that the results in the smart scenario are better than in the fixed scenario. In particular, the user's revenue objective, when the EV chooses the charging and discharging time according to the system intelligence, the user's revenue in the best compromise is increased by 48.1%, compared to the fixed scenario, and the best extreme is increased by 45.6%. Therefore, in V2G services, EVs choose smart charging and discharging modes, which not only can improve the user's income, but also reduce the fuel cost and pollution emission of the thermal power unit.

The arrival time of EVs at the workplace and the corresponding number of EVs can be calculated according to (1). The distribution of the first commute time and the number of 50,000 EVs are shown in Fig. 7. It can be seen from Fig. 7 that the travel time to work is between 04:00 and 12:00 and reaches a peak at 08:00. Besides, assume that EVs participating in V2G services complete a charge and discharge cycle within a period, and it is ensured that the SoC is 100% when using the EV for the first time each day. Figure 8 illustrates the SoC curves for two charging and discharging scenarios with different travel times. The solid black line in Fig. 8 represents the total SoC (tSoC) of all EVs in a period. The tSoC of the two scenarios can meet the changing trends of discharging during the peak load and charging in the valley. The difference is that in the smart scenario in Fig. 8a, the EVs have only one moment in a period, the SoC is 100, that is, the moment before travel. However, in the fixed scenario in Fig. 8b, because the charge and discharge time is fixed, it will appear that when the SoC is 100%, it has not yet reached another state (charging or discharging state). This results in multiple moments where the SoC is 100 in a period. Consequently, the user's revenue in the fixed scenario is less than in the smart scenario. These prove that the proposed DEED_EV

Table 5 The best compromise solutions obtained by MOEA/D-SS

| t	P_1	P_2	P_3	P_4	P_5	P_6	P_7	P_8	P_9	P_{10}	V2G	P_L	P_D
1	151.75	136.62	111.60	111.12	166.74	149.85	122.60	116.64	76.43	53.19	− 135.64	24.91	1036
2	151.97	142.83	146.15	140.11	208.01	156.50	129.81	119.42	79.27	53.76	− 187.45	30.39	1110
3	155.01	157.67	172.89	169.83	223.23	159.73	128.23	119.26	79.11	53.96	− 126.30	34.62	1258
4	164.59	181.59	194.92	219.35	242.72	160.00	130.00	119.91	80.00	55.00	− 100.80	41.27	1406
5	169.45	176.65	202.20	211.40	230.19	158.56	129.05	118.78	79.09	54.66	− 9.70	40.34	1480
6	218.56	229.74	230.81	224.88	223.91	159.59	129.89	120.00	79.23	55.00	5.32	48.93	1628
7	234.06	254.71	260.48	260.29	243.00	159.90	129.65	119.87	79.96	55.00	− 38.20	56.72	1702
8	252.00	274.16	287.36	283.05	242.80	159.85	129.72	119.78	79.73	54.80	− 44.66	62.59	1776
9	260.44	283.73	303.72	281.86	242.13	159.17	129.10	119.20	79.19	54.05	76.14	64.74	1924
10	279.64	285.45	305.07	299.05	243.00	159.99	130.00	119.95	79.98	55.00	132.81	67.94	2022
11	284.24	310.80	306.61	299.81	242.48	159.89	129.88	119.86	79.90	54.79	188.17	70.42	2106
12	291.31	309.90	325.82	300.00	243.00	160.00	130.00	120.00	80.00	55.00	184.34	72.38	2127
13	279.08	308.29	309.95	299.82	242.89	159.90	129.81	119.86	79.87	54.55	158.00	70.04	2072
14	257.97	284.71	302.84	299.33	242.58	159.79	129.81	119.80	79.72	54.80	58.57	65.94	1924
15	219.42	268.89	270.48	291.27	243.00	160.00	130.00	119.98	80.00	55.00	− 2.76	59.27	1776
16	197.93	219.67	255.21	255.82	242.95	159.94	129.99	119.94	80.00	54.99	− 111.26	51.18	1554
17	195.77	207.08	209.67	236.68	242.82	159.64	129.83	119.79	79.47	54.70	− 108.99	46.45	1480
18	237.30	237.72	244.87	224.67	225.54	160.00	130.00	120.00	80.00	55.00	− 35.36	51.73	1628
19	235.66	268.00	271.71	275.94	242.82	159.82	129.82	119.82	79.80	54.81	− 2.74	59.45	1776
20	254.60	281.87	298.57	299.69	242.87	159.85	129.98	119.98	79.87	54.98	115.01	65.26	1972
21	237.35	265.51	291.68	294.31	242.89	160.00	129.95	119.98	79.85	54.89	109.46	61.88	1924
22	208.33	230.17	252.37	237.98	242.97	159.96	129.94	119.96	79.97	54.97	− 37.23	51.40	1628
23	162.63	167.18	195.37	167.79	242.44	160.00	130.00	120.00	80.00	55.00	− 110.63	37.77	1332
24	150.49	136.15	131.60	141.38	176.52	157.39	129.17	118.31	79.19	54.80	− 62.96	28.02	1184
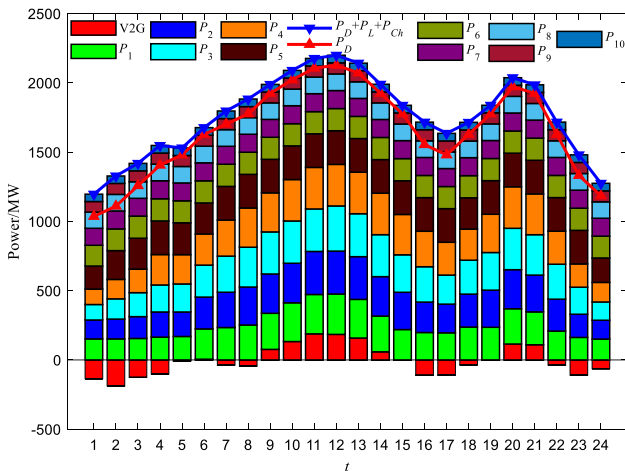
Fig. 6 Constraints checked MOEA/D-SS for the best compromise solutions

model, which generates the EVs charging and discharging scheme, can improve the user's revenue.

The most important role of EVs plugging into the power grid with V2G is to cut the peak and fill the valley of the system load. Figure 9 shows the profiles of load change when the system is plugged into the EVs in two scenarios. The gray areas represent the load reduced during peak load and the increase during the low valley, respectively. It can be seen from Fig. 9 that both scenarios can play the role of peak shaving and valley filling. In addition, in the smart scenario in Fig. 9a, the discharge power of EVs has reduced the load value in the peak areas of 08:00–15:00 and 19:00–22:00, respectively. These areas exactly match the peak areas (A and B) defined in Fig. 4. However, in the fixed scenario in Fig. 9b, the discharge power of EVs has reduced the load value in the peak areas of 08:00–14:00 and 17:00–22:00, respectively. But the 17:00–22:00 area contains part of the valley area, that is, the 17:00–19:00 area. Therefore, the peak shaving and valley filling performance of EVs in the fixed scenario is weaker than that of the smart scenario. This also proves that the proposed DEED_EV model can not only reduce the cost and emission of the thermal power unit but also have high peak shaving and valley filling performance.

Table 6 The results of the DEED_EV in smart and fixed scenarios

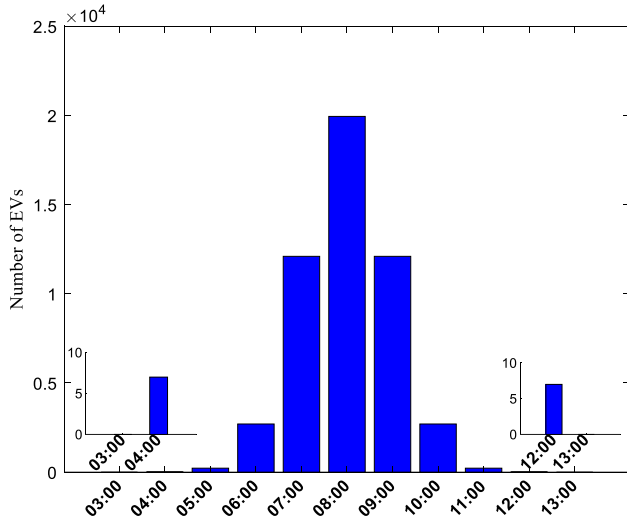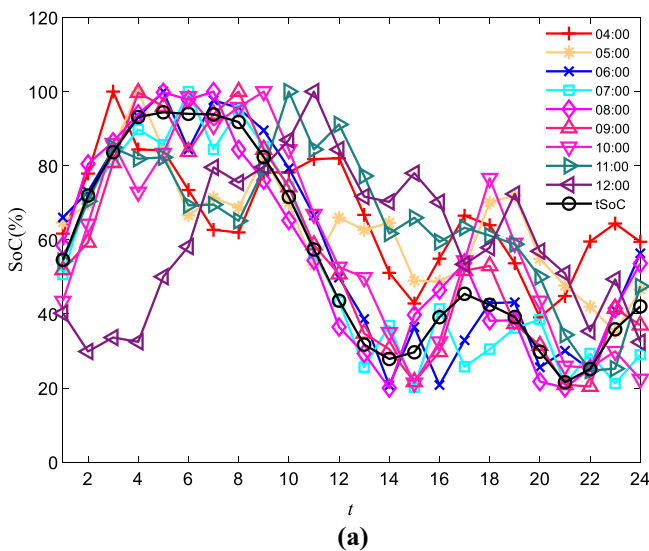| Scenario	Best extreme			Best compromise		
	Cost ($)	Emission (lb)	Revenue ($)	Cost ($)	Emission (lb)	Revenue ($)
Fixed	2.4348E + 06	2.8080E + 05	2.2169E + 05	2.4465E + 06	2.8388E + 05	2.2206E + 05
Smart	2.3916E + 06	2.7323E + 05	3.2271E + 05	2.4145E + 06	2.7913E + 05	3.2883E + 05

Fig. 7 The distribution of the arrival time and the number of EVs

4.3 Case 3

The battery capital cost C_{ev} is one of the factors that users should consider when buying an EV. Therefore, different C_{ev} from 200 to 800 is studied in this case. Table 7 lists the average values including three objective functions, EVs battery wear cost caused by V2G, and the battery wear cost of normal driving. And the change trends are shown in Fig. 10. It can be seen from Table 7 and Fig. 10 that the cost and emission of the thermal power unit have only slight changes when C_{ev} increases. Since the battery wears cost and drive wear cost are positively related to C_{ev}. Therefore, when C_{ev} increases, its corresponding battery wears cost and drive wear cost also increase. However, the user's revenue changes with C_{ev} are not monotonous. In Fig. 10, the user's revenue reaches the highest peak when C_{ev} is 500. In addition, as can be seen in Table 7, the use's revenue is much higher than wear cost and drive wear cost. Consequently, the wear of the battery in the proposed DEED_EV model is negligible for EVs plugged into V2G services. And the user can choose an EV with appropriate battery capital cost to ensure the best revenue when it is plugged into the grid.

4.4 Case 4

In the proposed DEED_EV model, the time-of-use electricity price is used to calculate the charging cost and
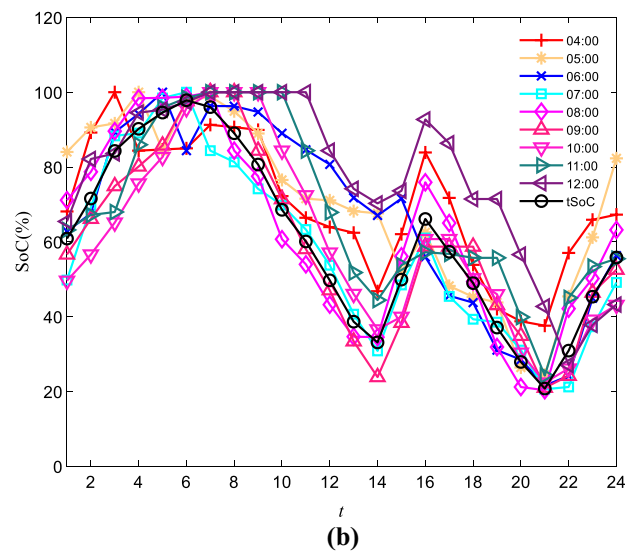

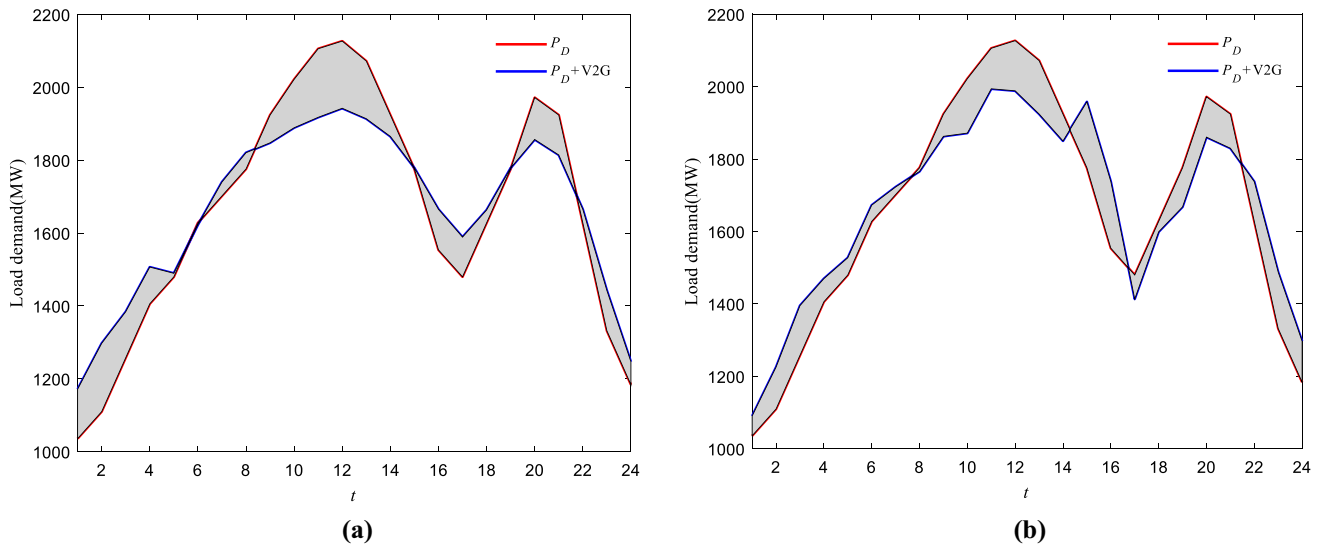**Fig. 8** SoC curves for different arrival times. **a** Smart scenario, and **b** fixed scenario

Fig. 9 Change profiles of system load demand in different scenarios. **a** Smart scenario and **b** fixed scenario

Table 7 The values of objective function under different battery capital costs

C_{ev}	Cost ($)	Emission (lb)	Revenue ($)	Wear cost ($)	Drive wear cost ($)
200	2.3968E + 06	2.7346E + 05	3.0983E + 05	17.82	4.71
300	2.3931E + 06	2.7333E + 05	3.1159E + 05	26.00	7.07
400	2.3924E + 06	2.7327E + 05	3.1422E + 05	35.05	9.42
500	2.3928E + 06	2.7307E + 05	3.1601E + 05	43.84	11.78
600	2.3943E + 06	2.7346E + 05	3.0153E + 05	52.71	14.14
700	2.3945E + 06	2.7339E + 05	3.1066E + 05	59.40	16.49
800	2.3942E + 06	2.7338E + 05	3.0509E + 05	70.62	18.85

discharging income. The time-of-use electricity price is shown in Fig. 4, in which the minimum $\text{Min}\pi_t$ is 17$/MW and the maximum $\text{Max}\pi_t$ is 572$/MW. In this case, the effect on the DEED_EV model is analyzed when the electricity prices are $0.1\pi_t$, $0.5\pi_t$, $1\pi_t$, $2\pi_t$, $\text{Min}\pi_t$, and $\text{Max}\pi_t$, respectively. The average values are listed in Table 8. The user's revenue is the highest when the electricity price is $2\pi_t$. But when the electricity price is fixed at $\text{Min}\pi_t$ (17$/MW) and $\text{Max}\pi_t$ (572$/MW), respectively, instead of the time-of-use price. The user's revenue only is 315.6996$ at $\text{Min}\pi_t$ and 6.6830E + 03$ at $\text{Max}\pi_t$, which is much lower than that of the time-of-use price.

In the cost objective, when the electricity price is $1\pi_t$, compared with $0.1\pi_t$, $0.5\pi_t$, and $2\pi_t$, the fuel cost of the thermal power unit is reduced by 0.021%, 0.076%, 0.088%, and only increased by 0.001% compared to $1.5\pi_t$. Besides, the fuel cost of the thermal power unit corresponding to the time-use-of electricity price is better than fixed prices $\text{Min}\pi_t$ and $\text{Max}\pi_t$. In the emission objective, the different emission of the thermal power unit in time-of-use prices is only reflected after the percentile. In addition, the emission in fixed prices $\text{Min}\pi_t$ and $\text{Max}\pi_t$ are increased by 6.34% and 3.00%, respectively, compared to $1\pi_t$. Therefore,

compared with the fixed price, the time-use-of price enables the EVs to get higher revenue by participating in the V2G services. Moreover, the higher the time-of-use price, the more the user's revenue.

5 Conclusions

In this paper, to promote the enthusiasm of users to participate in V2G services, considering the maximization of EV user's revenue, a new dynamic economic emission dispatch model with EVs (DEED_EV) is proposed for the minimum fuel cost and emission of the thermal power unit. In the DEED_EV, the travel randomness and battery wear of EVs users are considered. To quickly get the solutions into the decision space, a multi-objective method MOEA/D with a step-by-step constraint handling method (MOEA/D-SS) is developed. To verify the proposed model and method, four test cases based on the 10-unit are simulated, as well as the VEPSO, SaMODE_LS, NSDESa, and dNSGA-II are compared to MOEA/D-SS. The results show that the performance of MOEA/D-SS is better than VEPSO, SaMODE_LS, NSDESa, and dNSGA-II. In
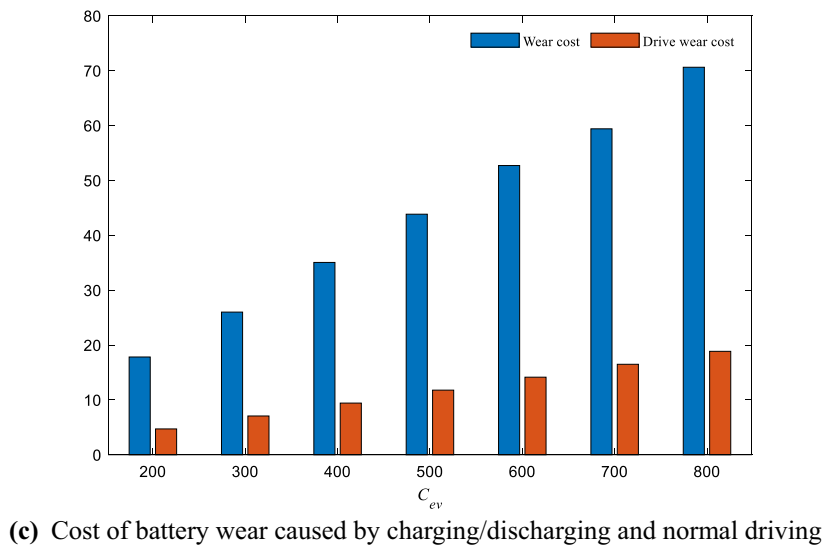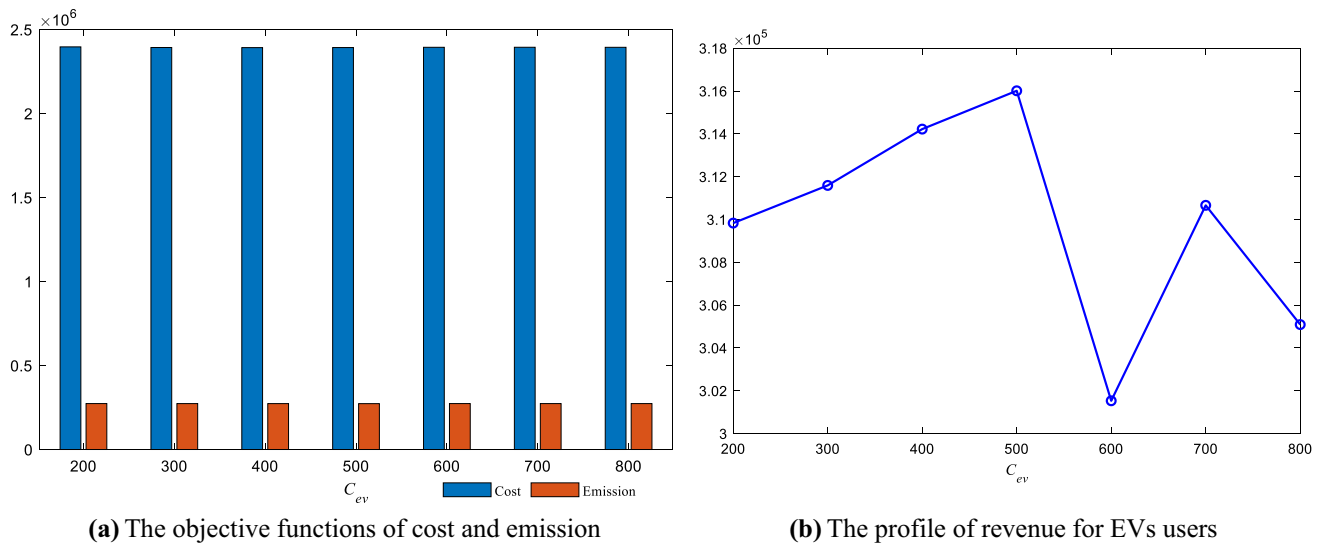
(a) The objective functions of cost and emission

(b) The profile of revenue for EVs users

(c) Cost of battery wear caused by charging/discharging and normal driving

Fig. 10 The changing trend of objective function under different battery capital costs

Table 8 Different electricity price

Electricity price	$0.1\pi_t$	$0.5\pi_t$	$1\pi_t$	$1.5\pi_t$	$2\pi_t$	$Min\pi_t$	$Max\pi_t$
Cost ($)	2.3933E + 06	2.3946E + 06	2.3928E + 06	2.3926E + 06	2.3949E + 06	2.4029E + 06	2.3997E + 06
Emission (lb)	2.7296E + 05	2.7326E + 05	2.7307E + 05	2.7378E + 05	2.7379E + 05	2.7539E + 05	2.7417E + 05
Revenue ($)	3.1030E + 04	1.5513E + 05	3.1601E + 05	4.5787E + 05	5.9859E + 05	315.6996	6.6830E + 03

addition, the DEED_EV model not only reduced the fuel cost and emission but also increased the revenue of EV users. Furthermore, the smart charging and discharging mode from the DEED_EV model is the best compared to the fixed mode, and the EVs fully realize the peak shaving and valley filling of the load. Moreover, the effect of battery capital cost on the DEED_EV is analyzed. The results show that the user's revenue is the highest when the battery

capital cost is 500$/kW. Finally, only by adopting a reasonable time-of-use electricity pricing strategy EV users can obtain higher revenues, thereby incentivizing more EV owners to add their EVs to V2G services. However, there are two major limitations in this study that can be addressed in future research. First, the study focused on a complete charging and discharging process of EVs in a dispatch cycle; that is, SoC changes from 100 to 0% and

then to 100%, but based on the psychological effect on users, they may not choose the V2G service when the power is still sufficient. Second, the study only considers thermal power units. With the development of low-carbon energy sources, renewable energy power will become the main power supply in the future. Therefore, in our future work, we will deeply study the influence of different SoCs of EVs, as well as the flexible interactive dispatching mechanism between renewable energy and EVs.

Data Availability Enquiries about data availability should be directed to the authors.

Declarations

Conflict of interests The authors declare no potential conflict of interests.

References

Admin (2021) Global EV outlook 2021. International energy agency. http://119.78.100.173/C666/handle/2XK7JSWQ/325044.

Al-Bahrani LT, Horan B, Seyedmahmoudian M, Stojcevski A (2020) Dynamic economic emission dispatch with load demand management for the load demand of electric vehicles during crest shaving and valley filling in smart cities environment. Energy. https://doi.org/10.1016/j.energy.2020.116946

Amjad S, Neelakrishnan S, Rudramoorthy R (2010) Review of design considerations and technological challenges for successful development and deployment of plug-in hybrid electric vehicles. Renew Sustain Energy Rev 14:1104–1110. https://doi.org/10.1016/j.rser.2009.11.001

Arul R, Velusami S, Ravi G (2015) A new algorithm for combined dynamic economic emission dispatch with security constraints. Energy 79:496–511. https://doi.org/10.1016/j.energy.2014.11.037

Azizipanah-Abarghooee R, Niknam T, Roosta A, Malekpour AR, Zare M (2012) Probabilistic multiobjective wind-thermal economic emission dispatch based on point estimated method. Energy 37:322–335. https://doi.org/10.1016/j.energy.2011.11.023

Basu M (2008) Dynamic economic emission dispatch using nondominated sorting genetic algorithm-II. Int J Electr Power Energy Syst 30:140–149. https://doi.org/10.1016/j.ijepes.2007.06.009

Basu M (2014) Fuel constrained economic emission dispatch using nondominated sorting genetic algorithm-II. Energy 78:649–664. https://doi.org/10.1016/j.energy.2014.10.052

Ding T, Bo R, Li FX, Gu Y, Guo QL, Sun HB (2015) Exact penalty function based constraint relaxation method for optimal power flow considering wind generation uncertainty. IEEE Trans Power Syst 30:1546–1547. https://doi.org/10.1109/TPWRS.2014.2341177

Farahani HF (2017) Improving voltage unbalance of low-voltage distribution networks using plug-in electric vehicles. J Clean Prod 148:336–346. https://doi.org/10.1016/j.jclepro.2017.01.178

Gonzalez-Castellanos A, Pozo D, Bischi A (2020) Detailed Li-ion battery characterization model for economic operation. Int J Electr Power Energy Syst. https://doi.org/10.1016/j.ijepes.2019.105561

Gopu A, Venkataraman N (2019) Optimal VM placement in distributed cloud environment using MOEA/D. Soft Comput 23:11277–11296. https://doi.org/10.1007/s00500-018-03686-6

Greeff M, Engelbrecht AP (2008) Solving dynamic multi-objective problems with vector evaluated particle swarm optimisation. In: 2008 IEEE congress on evolutionary computation (CEC), pp. 2917–2924. Doi: https://doi.org/10.1109/CEC.2008.4631190

Guo C, Zhan J, Wu Q (2012) Dynamic economic emission dispatch based on group search optimizer with multiple producers. Electr Power Syst Res 86:8–16. https://doi.org/10.1016/j.epsr.2011.11.015

Han XS, Gooi HB, Kirschen DS (2001) Dynamic economic dispatch: feasible and optimal solutions. IEEE Trans Power Syst 16:22–28. https://doi.org/10.1109/59.910777

Hu Z, Dai C, Su Q (2022) Adaptive backtracking search optimization algorithm with a dual-learning strategy for dynamic economic dispatch with valve-point effects. Energy. https://doi.org/10.1016/j.energy.2022.123558

Kalyanmoy D, Udaya BRN, Karthik S (2007) Dynamic multi-objective optimization and decision-making using modified NSGA-II: a case study on hydro-thermal power scheduling. In: International conference on evolutionary multi-criterion optimization, pp 803–817. Doi: https://doi.org/10.1007/978-3-540-70928-2_60

Kempton W, Letendre SE (1997) Electric vehicles as a new power source for electric utilities. Transp Res Part D Transp Environ 2:157–175. https://doi.org/10.1016/S1361-9209(97)00001-1

Li L-L, Liu Z-F, Tseng M-L, Zheng S-J, Lim MK (2021) Improved tunicate swarm algorithm: solving the dynamic economic emission dispatch problems. Appl Soft Comput 108:107504. https://doi.org/10.1016/j.asoc.2021.107504

Liang HJ, Liu YG, Li FZ, Shen YJ (2019) Dynamic economic/emission dispatch including PEVs for peak shaving and valley filling. IEEE Trans Ind Electron 66:2880–2890. https://doi.org/10.1109/TIE.2018.2850030

Lu X, Zhou K, Yang S (2017) Multi-objective optimal dispatch of microgrid containing electric vehicles. J Clean Prod 165:1572–1581. https://doi.org/10.1016/j.jclepro.2017.07.221

Lu X, Zhou K, Yang S, Liu H (2018) Multi-objective optimal load dispatch of microgrid with stochastic access of electric vehicles. J Clean Prod 195:187–199. https://doi.org/10.1016/j.jclepro.2018.05.190

Mason K, Duggan J, Howley E (2017) Multi-objective dynamic economic emission dispatch using particle swarm optimisation variants. Neurocomputing 270:188–197. https://doi.org/10.1016/j.neucom.2017.03.086

Mohiti M, Monsef H, Lesani H (2019) A decentralized robust model for coordinated operation of smart distribution network and electric vehicle aggregators. Int J Electr Power Energy Syst 104:853–867. https://doi.org/10.1016/j.ijepes.2018.07.054

NHTS (2017) National household travel survey. NHTS academy. https://nhts.ornl.gov/.

Niknam T, Azizipanah-Abarghooee R, Roosta A, Amiri B (2012) A new multi-objective reserve constrained combined heat and power dynamic economic emission dispatch. Energy 42:530–545. https://doi.org/10.1016/j.energy.2012.02.041

Nourianfar H, Abdi H (2019) Solving the multi-objective economic emission dispatch problems using fast non-dominated sorting

TVAC-PSO combined with EMA. Appl Soft Comput 85:105770. https://doi.org/10.1016/j.asoc.2019.105770

Peng MH, Lian L, Jiang CW (2012) A review on the economic dispatch and risk management of the large-scale plug-in electric vehicles (PHEVs)-penetrated power systems. Renew Sustain Energy Rev 16:1508–1515. https://doi.org/10.1016/j.rser.2011.12.009

Qiao BH, Liu J (2020) Multi-objective dynamic economic emission dispatch based on electric vehicles and wind power integrated system using differential evolution algorithm. Renew Energy 154:316–336. https://doi.org/10.1016/j.renene.2020.03.012

Qiao B, Liu J, Hao X (2021) A multi-objective differential evolution algorithm and a constraint handling mechanism based on variables proportion for dynamic economic emission dispatch problems. Appl Soft Comput 108:107419. https://doi.org/10.1016/j.asoc.2021.107419

Qiao B, Liu J (2021) Dynamic economic dispatch with electric vehicles considering battery wear cost using a particle swarm optimization algorithm. In: 2021 international conference on power system technology (POWERCON), IEEE, pp 807–813

Qu BY, Zhu YS, Jiao YC, Wu MY, Suganthan PN, Liang JJ (2018) A survey on multi-objective evolutionary algorithms for the solution of the environmental/economic dispatch problems. Swarm Evol Comput 38:1–11. https://doi.org/10.1016/j.swevo.2017.06.002

Qu BY, Qiao BH, Zhu YS, Jiao YC, Xiao JM, Wang XL (2017) Using multi-objective evolutionary algorithm to solve dynamic environment and economic dispatch with EVs. In: International conference on swarm intelligence (ICSI), pp 31–39. Doi: https://doi.org/10.1007/978-3-319-61833-3_4

Saber AY, Venayagamoorthy GK (2010) Intelligent unit commitment with vehicle-to-grid—a cost-emission optimization. J Power Sources 195:898–911. https://doi.org/10.1016/j.jpowsour.2009.08.035

Wang D, Coignard J, Zeng T, Zhang C, Saxena S (2016) Quantifying electric vehicle battery degradation from driving vs. vehicle-to-grid services. J Power Sources 332:193–203. https://doi.org/10.1016/j.jpowsour.2016.09.116

Wang G, Li X, Gao L, Li P (2021) Energy-efficient distributed heterogeneous welding flow shop scheduling problem using a modified MOEA/D. Swarm Evol Comput 62:100858. https://doi.org/10.1016/j.swevo.2021.100858

Xie Y, Yang S, Wang D, Qiao J, Yin B (2022) Dynamic transfer reference point oriented MOEA/D involving local objective-space knowledge. IEEE Trans Evol Comput. https://doi.org/10.1109/TEVC.2022.3140265

Xiong G, Shuai M, Hu X (2022) Combined heat and power economic emission dispatch using improved bare-bone multi-objective particle swarm optimization. Energy 123:1–8. https://doi.org/10.1016/j.energy.2022.123108

Xu X, Hu Z, Su Q, Xiong Z, Liu M (2021a) Multi-objective learning backtracking search algorithm for economic emission dispatch problem. Soft Comput 25:2433–2452. https://doi.org/10.1007/s00500-020-05312-w

Xu Z, Liu J, Qiao B, Cao Y (2021b) MOEA/D using dynamic weight vectors and stable matching schemes for the deployment of multiple airships in the earth observing system. In: 2021b IEEE congress on evolutionary computation (CEC), IEEE, pp 177–184

Yang ZL, Li K, Niu Q, Xue YS, Foley A (2014) A self-learning TLBO based dynamic economic/environmental dispatch considering multiple plug-in electric vehicle loads. J Mod Power Syst Clean Energy 2:298–307. https://doi.org/10.1007/s40565-014-0087-6

Zakariazadeh A, Jadid S, Siano P (2014) Multi-objective scheduling of electric vehicles in smart distribution system. Energy Convers Manag 79:43–53. https://doi.org/10.1016/j.enconman.2013.11.042

Zhang QF, Li H (2007) MOEA/D: a multiobjective evolutionary algorithm based on decomposition. IEEE Trans Evol Comput 11:712–731. https://doi.org/10.1109/TEVC.2007.892759

Zhang H, Yue D, Xie X, Hu S, Weng S (2015) Multi-elite guide hybrid differential evolution with simulated annealing technique for dynamic economic emission dispatch. Appl Soft Comput 34:312–323. https://doi.org/10.1016/j.asoc.2015.05.012

Zhang X, Wang Z, Lu Z (2022) Multi-objective load dispatch for microgrid with electric vehicles using modified gravitational search and particle swarm optimization algorithm. Appl Energy 306:118018. https://doi.org/10.1016/j.apenergy.2021.118018

Zhou CK, Qian KJ, Allan M, Zhou WJ (2011) Modeling of the cost of EV battery wear due to V2G application in power systems. IEEE Trans Energy Convers 26:1041–1050. https://doi.org/10.1109/TEC.2011.2159977

Zhu YS, Qiao BH, Dong Y, Qu BY, Wu DY (2019) Multiobjective dynamic economic emission dispatch using evolutionary algorithm based on decomposition. IEEJ Trans Electr Electron Eng 14:1323–1333. https://doi.org/10.1002/tee.22933